

X-ray diffraction study of the optimization of MgO growth conditions for magnetic tunnel junctions

Se Young O,^{1,2} Chan-Gyu Lee,² Alexander J. Shapiro,¹ William F. Egelhoff, Jr.,^{1,a)} Mark D. Vaudin,³ Jennifer L. Ruglovsky,³ Jonathan Mallett,¹ and Philip W. T. Pong^{1,b)}

¹Magnetic Materials Group, National Institute of Standards and Technology, Gaithersburg, Maryland 20899, USA

²School of Nano and Advanced Materials Engineering, Changwon National University, 9 Sarim-dong, Changwon, Gyeongnam 641-773, Republic of Korea

³Ceramic Division, National Institute of Standards and Technology, Gaithersburg, Maryland 20899, USA

(Presented on 9 November 2007; received 11 September 2007; accepted 3 November 2007; published online 14 April 2008)

We have carried out a systematic study optimizing the MgO growth via preparation and sputtering conditions and underlayer structures. It was found that to prevent water vapor which is detrimental to MgO (200) growth, the chamber pressure needs to be reduced below 10^{-8} Torr. Simple underlayers such as 5 nm CoFeB tend to give better MgO, but we have also succeeded in growing MgO on more complicated underlayers such as 1 Ta/20 Au/5 Co₄₀Fe₄₀B₂₀ and 1 Ta/20 conetic (Ni₇₇Fe₁₄Cu₅Mo₄)/1.5 Co₄₀Fe₄₀B₂₀ (units in nanometers). We accomplished this by extensive baking of the deposition chamber and use of Ti-getter films. Short sputtering distance and high sputtering power were found to optimize MgO deposition. We found that both preparation and sputtering conditions have important effects on the MgO growth. X-ray diffraction analysis was used as the characterization tool for optimizing the MgO growth conditions. © 2008 American Institute of Physics. [DOI: 10.1063/1.2836405]

I. INTRODUCTION

Theoretical prediction has indicated that the crystallinity of the MgO tunnel barrier in magnetic tunnel junctions (MTJs) could provide tunneling magnetoresistance (TMR) ratios as high as 6000% because of the coherent tunneling properties for such a junction system.¹⁻³ Recently, there are reports showing MTJs made with MgO (200) exhibiting even higher TMR of 400%–500%.⁴⁻⁶ Therefore, the crystalline MgO (200) tunnel barrier is the key to achieving good MR ratios.

In this paper, we studied the influences of several different preparations and sputtering conditions on the MgO growth by x-ray diffraction (XRD) analysis.

II. EXPERIMENT

The thin films were deposited on Si (100)/1500 SiO₂ wafer (units in nanometers) by magnetron sputtering in an ultrahigh vacuum chamber with a base pressure of 2×10^{-10} Torr and a working pressure of 2×10^{-3} Torr argon. Titanium gettering was performed to pump down the chamber before sputter deposition of each sample. The metal films were deposited at room temperature by dc magnetron sputtering in argon. The MgO oxide layer was deposited by rf magnetron sputtering from a MgO target. Unless specified, the sample structures were substrate/5 Co₄₀Fe₄₀B₂₀/30 MgO (units in nanometers). The samples were characterized by x-ray diffraction (XRD) theta-two theta measurements (D8

DISCOVER, Bruker AXS). *XRD patterns were taken with the Bruker AXS system* equipped a crossed-wire area (two-dimensional) detector. In the measurement, the scattering intensity was measured over a range of $25^\circ < 2\theta < 60^\circ$ with the detector held fixed, while the sample was rotated continuously through the range of $21.2^\circ < \omega < 21.7^\circ$. The resulting spectra were integrated over the range of $-67^\circ < \chi < -111^\circ$ to provide a single graph of integrated intensity versus 2θ . The rocking curves were obtained by integrating over the range of $43.2^\circ < 2\theta < 44.8^\circ$. XRD spectrum was collected for each sample at ambient temperature using Cu K α radiation for a time frame of 30 min. Peak height data were measured as peak heights above the background.

III. RESULTS AND DISCUSSION

A. Preparation conditions

1. Bakeout temperature

A vacuum chamber is usually baked before use to remove impurity gases and water molecules. Our sputtering chamber (without substrate) was baked at two separate times at 80 and 175 °C, respectively, for 12 h. After 80 °C baking, the chamber pressure was around 2×10^{-8} Torr. After 175 °C baking, the chamber pressure was about 2×10^{-10} Torr. We compared the samples made after the 80 and 175 °C bakeouts (substrates were loaded into the chamber after bakeouts) in order to understand the influence of the bakeout temperature. One typical comparison result is shown in Fig. 1(a). The samples made after 175 °C baking exhibit much better XRD results as evidenced by MgO (200) peaks that are much more consistent and pronounced. The enhancement appears to be due to the better chamber pressure. A

^{a)}Electronic mail: william.egelhoff@nist.gov.

^{b)}Author to whom correspondence should be addressed. Electronic mail: ppong@nist.gov.

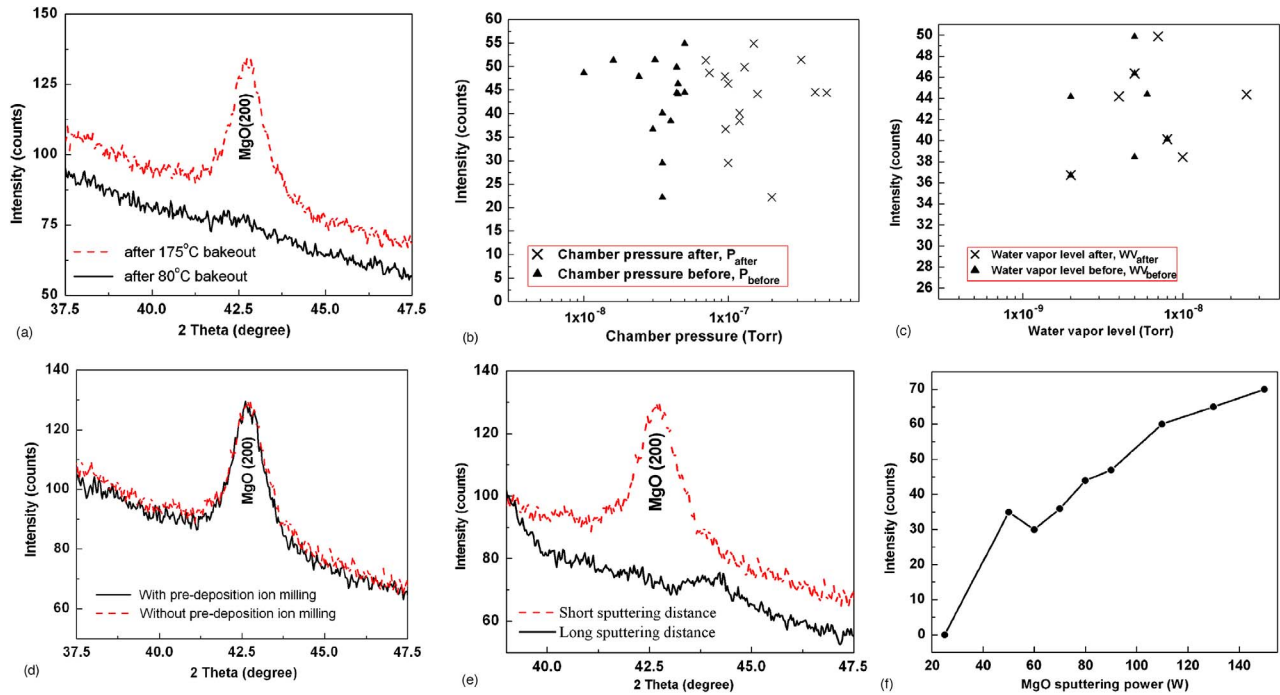


FIG. 1. (Color online) (a) The typical XRD spectra of the samples made after different bakeout temperatures. The samples made after 175 °C bakeout show a pronounced MgO (200) peak. (b) After high temperature bakeout, no correlation was found between the intensity of the MgO (200) peak and the chamber pressure before opening the argon leak valve and the chamber pressure 2 min after the argon leak valve was closed. (c) After high temperature bakeout, no correlation was found between the intensity of the MgO (200) peak and the water vapor level. The water vapor level before was measured before opening the argon leak valve and the water vapor level after was measured 2 min after the argon leak valve was closed. (d) XRD pattern comparison between two representative samples made with and without predeposition ion milling. (e) XRD pattern comparison between samples made at short sputtering distance of 3.8 cm and samples made at long sputtering distance of 17.8 cm. (f) The relationship between the intensity of the MgO (200) peak and the sputtering power.

chamber with lower pressure contains less impurity gases and water vapor and therefore it provides a cleaner environment for deposition. The experimental results show that a high temperature bakeout improves the crystalline MgO (200) structure.

2. Chamber pressure and water vapor level

Based on the result in Sec. I, the sputtering chamber (without substrate) was baked at 175 °C for 12 h and the base pressure was 2×10^{-10} Torr. To further investigate how chamber pressure and water vapor level affect MgO growth, samples with varying parameters: chamber pressure (P_{before}), water vapor level (WV_{before}) before sputtering (i.e., before letting argon gas in), the chamber pressure (P_{after}), water vapor level (WV_{after}) after sputtering (i.e., after argon leak valve is closed) were measured. The water vapor level was measured by a residual gas analyzer and is expressed as pressure here. The P_{before} and P_{after} were within small ranges (for P_{before} , mean= 3.6×10^{-8} Torr, standard deviation= 1.2×10^{-8} Torr; for P_{after} , mean= 1.7×10^{-7} Torr, standard deviation= 1.3×10^{-7} Torr) in order to investigate closely how small changes on the chamber pressure will affect the MgO growth. For the similar reason, the WV_{before} and WV_{after} were also within small ranges (for WV_{before} , mean= 4.7×10^{-9} Torr, standard deviation= 2.1×10^{-9} Torr; for WV_{after} , mean= 8.7×10^{-9} Torr, standard deviation= 7.7×10^{-9} Torr). Figure 1(b) shows the plot of the MgO (200) peak heights of these samples versus P_{before} and P_{after} . There are no obvious correlations between the peak heights and the

P_{before} , and P_{after} . Apparently, after reducing the chamber pressure to a critically low level of around 2×10^{-10} Torr, the chamber pressure is no longer the dominating factor to the MgO (200) growth; in that pressure range, small fluctuations of the chamber pressure have minimal effect on the MgO deposition. Figure 1(c) shows the plot of the MgO (200) peak heights versus WV_{before} and WV_{after} . There are no obvious correlations between the peak heights and the WV_{before} and WV_{after} . This result indicates that by baking the sputtering chamber at 175 °C for 12 h, the water vapor is greatly minimized to a low level that it no longer inhibits the MgO (200) formation.

3. Predeposition ion milling

Predeposition ion milling is commonly used to clean contaminants off a substrate surface before MTJ thin films are deposited. Here, we studied its effect on the MgO growth. Before sputter deposition, the Si/SiO₂ wafer was ion milled with argon ions to remove ~ 5 nm of SiO₂ to clean the surface for subsequent MgO growth. Figure 1(d) shows the typical XRD spectra of samples made with and without predeposition ion milling. Predeposition ion milling cleaning of the thermal-oxide substrate before depositing metal films does not improve the subsequent MgO crystal growth. In general, the samples made without predeposition ion milling exhibit similar MgO (200) peak heights as the samples made with predeposition ion milling. It is probably because CoFeB

is amorphous that the substrate condition does not matter to the subsequent MgO growth because the memory of the substrate is lost after 5 nm CoFeB is deposited.

B. Sputtering conditions

Based on the result of Sec. III A 1, the investigations in this section were carried out after the sputtering chamber (without substrate) was baked at 175 °C for 12 h and the base pressure was 2×10^{-10} Torr. The MgO thicknesses for all the samples were 30 nm. The difference in the sputtering rate due to different sputtering distances and different sputtering powers were taken into account by using appropriate sputtering time.

1. Sputtering distance

We studied the dependence of the MgO (200) structure on the sputtering distance. Comparing the normal sputtering distance of around 17.8 cm with a very close sputtering distance of around 3.8 cm, we did not observe any MgO (200) peaks for the long sputtering distance case, whereas the MgO (200) peaks were shown for the short sputtering distance case. The typical results for the two cases are shown in Fig. 1(e). The samples made with the sputtering distance of around 3.8 cm showed strong intensity of the MgO (200) peak. We believe that the short sputtering distance greatly reduces the exposure of the growing MgO film to contaminants; the most notable contaminant suspect being water vapor as MgO is hygroscopic.

2. Sputtering power

We investigated the dependence of the MgO (200) crystallinity on the MgO sputtering power. The deposition of MgO layer at rf magnetron power from 25 to 150 W systematically resulted in increasingly intense (200) oriented MgO, as shown in Fig. 1(f). The intensity of the MgO peak at 150 W is around twice as that at 50 W. A higher sputtering power increases the MgO deposition rate, and therefore it reduces the exposure of the growing MgO film to contaminants. Also, we can explain this trend by inspection of the MgO (200) rocking curve. There is an approximately 5% narrowing in out-of-plane texture with the highest sputtering power versus the lowest. The sputtering power has an important effect on the formation of high quality MgO.

3. Different underlayer structures

A realistic MTJ structure usually involves more than CoFeB as the underlayer. Therefore, the above optimized preparation and sputtering conditions were used to deposit MgO with more complicated underlayer structures: (1) substrate/1 Ta/20 conetic ($\text{Ni}_{77}\text{Fe}_{14}\text{Cu}_5\text{Mo}_4$)/1.5 $\text{Co}_{40}\text{Fe}_{40}\text{B}_{20}$ /30 MgO, (2) substrate/1 Ta/10 Au/5 $\text{Co}_{40}\text{Fe}_{40}\text{B}_{20}$ /30 MgO, and (3) substrate/1 Ta/20 Au/5 $\text{Co}_{40}\text{Fe}_{40}\text{B}_{20}$ /30 MgO (units in nanometers). In general,

MgO samples with simple structures [substrate/5 $\text{Co}_{40}\text{Fe}_{40}\text{B}_{20}$ /30 MgO (units in nanometers)] show MgO (200) peak heights of around 40 counts and full width at half maximum (FWHM) of the rocking curve of around 7°. XRD spectrum on sample (1) shows that significant progress was made toward depositing good MgO on conetic and $\text{Co}_{40}\text{Fe}_{40}\text{B}_{20}$. The MgO (200) peak height is 37.2 counts and the FWHM of the rocking curve is 9.6°. We also included a Au underlayer in sample (2) and succeeded in making MgO (200) on top of substrate/1 Ta/10 Au/5 $\text{Co}_{40}\text{Fe}_{40}\text{B}_{20}$. It exhibited a MgO (200) peak height of 29.8 counts and FWHM of the rocking curve of 7.9°. Sample (3) has a thicker 20 nm Au underlayer and the MgO (200) structure remained. The sample showed the MgO (200) peak height of 21.7 counts and FWHM of the rocking curve of 8.18°. These results show that the above optimized preparation and sputtering conditions are not limited to the simple substrate/5 $\text{Co}_{40}\text{Fe}_{40}\text{B}_{20}$ /30 MgO structure; the conditions are extensible to more complicated underlayer structures as well.

IV. CONCLUSION

Both preparation and sputtering conditions have important effect on the MgO growth. In order to obtain highly crystalline MgO (200) structure, the preparation and sputtering conditions have to be optimized. For the preparation conditions, high temperature baking and extensive use of Ti-getter films reduce the chamber pressure and water vapor to the lowest possible level which is critical to the formation of MgO (200) layer. Small fluctuations in the chamber pressure and water vapor level do not seem to affect the MgO crystallinity at very low chamber base pressure of around 10^{-10} Torr. Predeposition ion milling to clean the thermal-oxide substrate before depositing metal films is not necessary for the subsequent MgO crystal growth. For the sputtering conditions, short sputtering distance and high sputtering power are crucial for the formation of good MgO. The optimized preparation and sputtering conditions are applicable for simple and more complicated underlayer structures.

**Note added in proof.* Certain commercial equipment, instruments, or materials are identified in this document to specify the experimental conditions. Such identification does not imply recommendation or endorsement by the National Institute of Standards and Technology, nor does it imply that the products identified are necessarily the best available for the purpose.

¹W. H. Butler, X.-G. Zhang, T. C. Schulthess, and J. M. MacLaren, *Phys. Rev. B* **63**, 054416 (2001).

²J. Mathon and A. Umersky, *Phys. Rev. B* **63**, 220403 (2001).

³X.-G. Zhang and W. H. Butler, *Phys. Rev. B* **70**, 172407 (2004).

⁴S. S. P. Parkin, C. Kaise, A. Panchula, P. M. Rice, B. Hughes, M. Samant, and S.-H. Yang, *Nat. Mater.* **3**, 862 (2004).

⁵S. Yuasa, T. Nagahama, A. Fukushima, Y. Shzuki, and K. Ando, *Nat. Mater.* **2**, 868 (2004).

⁶J. Hayakawa, S. Ikeda, Y. M. Lee, F. Matsukura, and H. Ohno, *Appl. Phys. Lett.* **89**, 232510 (2006).